ISBN: 978-3-95450-231-8 ISSN: 2673-5490 doi: 10.18429/JACoW-IPAC2023-MOPA051

NONLINEAR COUPLING RESONANCES IN THE EIC ELECTRON STORAGE RING*

M. G. Signorelli† [1], G. H. Hoffstaetter[1,2], D. Sagan[1]
[1]Cornell University, Ithaca, NY, USA
[2]Brookhaven National Laboratory, Upton, NY, USA

Abstract

The 18 GeV Electron Storage Ring (ESR) lattice of the Electron-Ion Collider (EIC) showed various undesirable effects in nonlinear Monte Carlo tracking, including a vertical core emittance exceeding radiation-integral predictions and a low asymptotic polarization. These problems were resolved in a newer lattice where dispersion in the solenoidal spin rotators was set to zero. Here we identify the cause of the effects as a 2nd order synchro-beta resonance which is driven by vertical dispersion in the quadrupoles of the rotators. The 5 and 10 GeV ESR lattices have small but nonzero dispersion in the rotators, and misalignments in the 18 GeV case will inevitably create some dispersion, so care must be taken that this 2nd order resonance is not excited. Zero dispersion in the spin rotators may therefore not be the best solution, and a new working point is sought that is not close to this resonance. The implications of this result on the design of the ESR – including achieving a longitudinal spin match – are explored.

INTRODUCTION

The design of the Electron Storage Ring (ESR) of the Electron-Ion Collider to be built at Brookhaven National Laboratory is currently ongoing. Iterative analyses of dynamic aperture, polarization, and beam-beam effects are occurring concurrently with the release of each new lattice version. Last year, we published Monte Carlo tracking results of the 18 GeV ESR lattice showing a significant disagreement of the nonlinear polarization and vertical emittance with analytical calculations [1]. Difficulties with the dynamic aperture were also found [2]. These effects were resolved in a newer version which had removed dispersion in the solenoidal spin rotators by turning off the short solenoid module, where dispersion cannot be suppressed, and suppressing dispersion in the long solenoid module. Figure 1 shows an example of a solenoid "module".

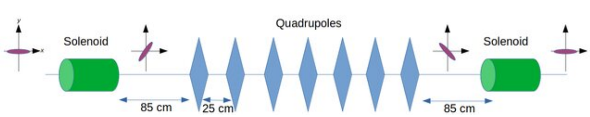

Figure 1: Solenoid "module" - two solenoids separated by quadrupoles for decoupling and spin matching [3].

Understanding the cause of the negative effects is necessary to ensure the new solution is sufficient and robust. Furthermore, by turning off the short solenoid module, the longitudinal spin match is lost and polarization is reduced [4]. In this work, we use various Monte Carlo tracking methods to identify the cause as a 2nd order synchro-beta resonance excited by vertical dispersion in quadrupoles.

METHODS

In this paper, long term tracking is done using the *long_term_tracking* program, which is part of the Bmad ecosystem of programs. Bmad [5] is a toolkit (software library) for charged particle and X-ray simulations in accelerators and storage rings. Lattice manipulation used the *Tao* [6] program which is also part of the Bmad ecosystem.

All Monte Carlo tracking results include radiation damping and fluctuations. The `taper` command in the *Tao* program was used to fix the closed orbit sawtooth effect due to radiation. *Map Tracking* uses truncated Taylor series maps which include spin transport. The truncation order is user-specified. With map tracking, radiation effects are applied at the bend centers and maps are used to transport the beam from bend center to bend center. *Bmad Tracking* uses fully nonlinear, element-by-element tracking unless otherwise specified. *PTC Tracking* is element-by-element symplectic integration using the PTC toolkit [7]. Both Bmad tracking and PTC tracking apply radiation effects step-by-step. The emittances obtained from tracking are the bunch eigen-emittances calculated from the 6D beam distribution. The three normal modes labeled "a", "b", and "c" correspond to the horizontal-like, vertical-like, and longitudinal-like modes [8]. Radiation-integral calculations generalized for a coupled lattice are used to calculate the equilibrium emittances. All tracking reported here use 5,000 to 10,000 particles, with an initial 6D distribution equal to the analytical equilibrium beam distribution.

RESULTS AND DISCUSSION

Table 1 shows the RMS equilibrium emittances obtained from various tracking methods versus the analytical calculation. While $\epsilon_{a,\mathrm{RMS}}$ shows good agreement in the fully nonlinear case, $\epsilon_{b,\mathrm{RMS}}$ significantly exceeds the linear prediction.

Core Emittance

Because the ESR is a nonlinear ring with high strength solenoids and sextupoles, one suspicion was that the nonlinearities were driving the tails of the distribution in the

* Work supported by Brookhaven Science Associates, LLC under Contract No. DESC0012704 with the U.S. Department of Energy, by National Science Foundation award number DMR-1829070, and by DOE award DE-SC0018370.
† mgs255@cornell.edu

ISBN: 978-3-95450-231-8 ISSN: 2673-5490 doi: 10.18429/JACoW-IPAC2023-MOPA051

Table 1: RMS emittances for an 18 GeV ESR lattice with fractional tunes $(Q_x, Q_y, Q_s) = (0.12, 0.10, 0.05)$.

	$\epsilon_{\mathrm{a,RMS}}$ [nm]	$\epsilon_{\mathrm{b,RMS}}$ [nm]
Analytical	27.7	~ 0
1st Order Map Tracking	27.7	~ 0
2nd Order Map Tracking	31.4	2.4
3rd Order Map Tracking	28.9	10.6
Bmad Tracking	28.7	12.3
PTC Tracking	28.8	12.3

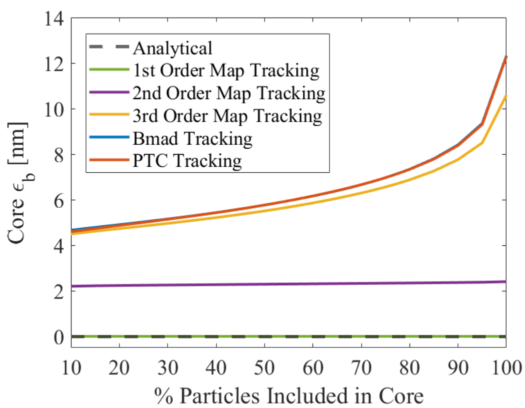

Figure 2: Vertical (b-mode) core emittances for varying percents of particles included in the core for an 18 GeV ESR lattice with fractional tunes $(Q_x, Q_y, Q_s) = (0.12, 0.10, 0.05)$. The Bmad Tracking line is almost identical with the PTC Tracking line and so is indistinguishable.

vertical to large amplitudes. In such a case, the RMS emittance is not the best measure of the beam distribution. Rather, the *core emittance* should be used. There are various definitions of a core emittance in the literature [9]. In this paper, the core emittance for a given mode and a given core size (expressed as some percentage of the total number of particles) is calculated using the following algorithm: the particles with the largest amplitudes for the given mode are removed until the percentage of particles left matches the given core size. The eigenmodes are then recalculated, and, starting with the entire beam, the removal process is repeated. A Gaussian is then fit to this final core distribution, giving the core emittance. This algorithm is called the "non-combined core emittance" calculation and is detailed in the *long_term_tracking* program manual [10]. With this definition, a perfectly Gaussian distribution would yield the same core emittance regardless of the cutoff amplitude. Near 0% only particles near the center of the beam are included and at 100% the full beam is included.

Figure 2 shows the vertical core emittances as a function of the number of particles included in the core. For the tracking that includes the most nonlinear effects (Bmad, PTC and 3rd order map tracking) ϵ_b is about 5 nm which is significantly larger than the linear radiation-integral prediction. It should

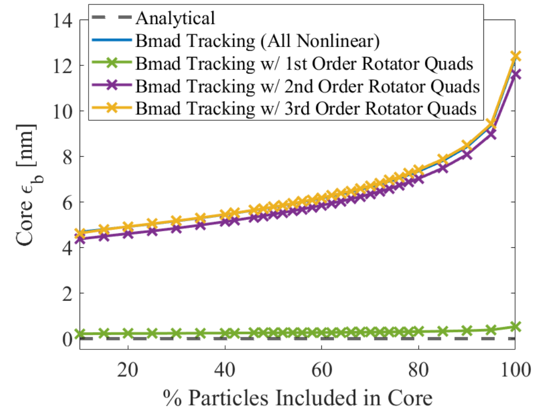

Figure 3: Vertical (b-mode) core emittances for the 18 GeV ESR with varying order map tracking through the rotator quadrupoles but fully nonlinear in the rest of the ring.

be noted that for 2nd order tracking the distribution remains Gaussian (the core emittance is constant regardless of cutoff percent). However, $\epsilon_b \approx 2$ nm in this case. This strongly suggests that there is some nonlinear effect present that blows up the beam vertically even in the core.

Source of Effects

For the lattice used for tracking, which has a longitudinal spin match, vertical enlargement could only be generated by nonlinear coupling effects. There are several possible causes including nonlinear effects in the solenoids and/or quadrupoles in the solenoid modules where there is localized coupling, as well as closed orbit deviations through the sextupoles due to radiation. To narrow down the exact element(s) and order at which the effect becomes most prominent, nonlinear Bmad tracking was performed except at select elements, where tracking was done with 1st, 2nd, or 3rd order Taylor maps. Figure 3 shows the core ϵ_b where only the quadrupoles in between the solenoids ("rotator quads") are tracked with varying order maps, and the rest of the ring is fully nonlinear including the solenoids. The full effect presents once 2nd order orbit motion in the quadrupoles between the solenoids is included in the tracking. Notably, this effect was not observed if the dispersion entering the solenoid module was made to be zero.

Identification of Resonance

A sweep of the synchrotron tune Q_s reveals a 2nd order resonance as shown in Figure 4. This figure shows the 80% core ϵ_b obtained from 3rd order map tracking as a function of Q_s. As a control, each of the core ϵ_b obtained with 1st order map tracking was verified with the linear calculation. As shown, there is a spike in ϵ_b at the current working point (WP) of $Q_s = 0.05$. This peak is at the $Q_y - 2Q_s$ 2nd order synchro-beta resonance. The polarization shows similar results; Figure 5 shows the average bunch replacement time to maintain a time-averaged polarization of no less than 70% for each bunch vs. Q_s.

ISBN: 978-3-95450-231-8 ISSN: 2673-5490 doi: 10.18429/JACoW-IPAC2023-MOPA051

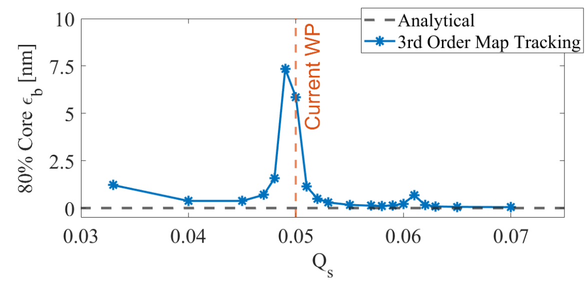

Figure 4: 80% core ϵ_b obtained from 3[rd] order map tracking for varying Q_s with constant $(Q_x, Q_y) = (0.12, 0.10)$.

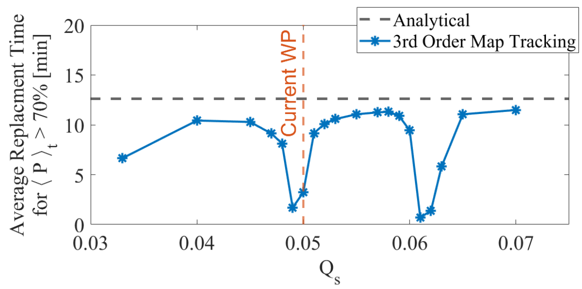

Figure 5: Average bunch replacement time for sufficient polarization vs. Q_s with constant $(Q_x, Q_y) = (0.12, 0.10)$.

The driving term for the $Q_y - 2Q_s$ resonance in quadrupoles can be obtained from the $e^{i(Q_y-2Q_s+n)\theta}$ coefficient in the quadrupole Hamiltonian after power series expansion in Floquet variables. Equivalently, in betatron-dispersion form we look for terms proportional to $y_\beta \delta^2$, where y_β is the energy-independent, vertical betatron oscillation and $\delta = \Delta p / p_0$.

$$
\begin{aligned}
H &= \frac{1}{2} K \left(x^2 - y^2\right) \\
&\approx \frac{1}{2} \frac{K_0}{1+\delta} \left((x_\beta + \eta_x \delta)^2 - (y_\beta + \eta_y \delta)^2\right) + \ldots \\
&\approx K_0 \eta_y y_\beta \delta^2 + \ldots
\end{aligned} \tag{1}
$$

The driving term for the $Q_y - 2Q_s$ resonance is $K_0 \eta_y$, where K_0 is the nominal quadrupole strength and η_y is the vertical dispersion. This solves the mystery. The only places in the ring where there is vertical dispersion in quadrupoles are the rotator quadrupoles when nonzero horizontal dispersion enters the solenoid module. The horizontal dispersion is locally coupled into the vertical within a solenoid module, thus exciting the resonance in the decoupling quadrupoles.

While the undesirable effects can be removed by zeroing dispersion entering each solenoid, with misalignments this is not fully achievable. And, because dispersion cannot be suppressed in the short solenoid module, the short solenoids must be turned off and the longitudinal spin match dropped. As shown in Fig. 5, when sufficiently off resonance, excellent polarization is achievable. Finally, both the 5 and 10 GeV ESR lattices have small but nonzero dispersion in the solenoids. Thus, a new working point must be determined.

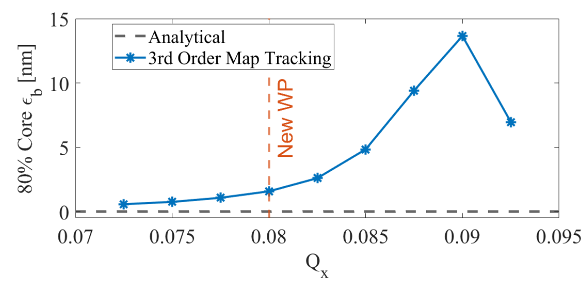

Figure 6: 80% core ϵ_b obtained from 3[rd] order map tracking for varying Q_x with $Q_s = 0.05$ and $Q_y = 0.14$.

New Tunes

Changing Q_s to avoid the resonance is not possible due to strict requirements on the RF bucket size. Beam-beam simulations suggested a new fractional tunes of $(Q_x, Q_y) = (0.08, 0.14)$. These tunes were implemented in the ESR lattice presented in this work by varying the arc quadrupoles. Figure 6 shows the 80% core ϵ_b for constant $Q_s = 0.05$ and $Q_y = 0.14$, but now varying Q_x. Again, as a control, the core emittances calculated from tracking using a 1[st] order map corresponded well with the linear calculation.

For these new tunes, the $Q_y - Q_s - Q_x$ resonance is particularly apparent. While not shown here, the 80% core ϵ_a vs. Q_x plot shows the same trend but decreasing near $Q_x = 0.09$ instead of increasing. This lattice, however, has the same sextupole settings optimized for the original $(0.12, 0.10)$ fractional tunes; with new settings, this effect will likely be suppressed. This shows the importance of iteratively selecting a new WP while considering all of beam-beam effects, dynamic aperture, and polarization.

CONCLUSIONS

The cause of various undesirable effects observed in the 18 GeV ESR lattice - including low asymptotic polarization, ϵ_b exceeding radiation-integral predictions, and dynamic aperture difficulties - was determined to be the $Q_y - 2Q_s$ 2[nd] order synchro-beta resonance, excited by vertical dispersion in decoupling quadrupoles. Because misalignments will inevitably create some vertical dispersion, and the 5 and 10 GeV ESR lattices have nonzero dispersion entering the solenoid modules where it is coupled into the vertical, this resonance must be avoided. Dispersion therefore is allowable in the solenoid modules. The short solenoid module no longer needs to be turned off, and a longitudinal spin match may be possible. When sufficiently away from this resonance, excellent polarization is observed in the 18 GeV ESR lattice with longitudinal spin matching. Finally, Monte Carlo tracking results of a new working point with fractional tunes $(Q_x, Q_y) = (0.08, 0.14)$ were shown for the same ESR lattice, where significant effects of another synchro-beta resonance $Q_y - Q_s - Q_x$ were apparent. However, with optimized sextupole settings for the new tunes, these effects are expected to be significantly suppressed.

ISBN: 978-3-95450-231-8 ISSN: 2673-5490 doi: 10.18429/JACoW-IPAC2023-MOPA051

REFERENCES

[1] M. G. Signorelli, G. H. Hoffstaetter, J. Kewisch, and J. A. Crittenden, "Spin Matching for the EIC's Electrons," in *Proc. IPAC'22*, Bangkok, Thailand, 2022, pp. 2369–2372. doi:10.18429/JACoW-IPAC2022-WEPOMS051

[2] D. Marx *et al.*, "Dynamic aperture optimization in the EIC electron storage ring with two interaction points," in *Proc. IPAC'21*, Campinas, Brazil, 2021, pp. 1984–1987. doi:10.18429/JACoW-IPAC2021-TUPAB235

[3] D. Marx *et al.*, "Designing the EIC Electron Storage Ring Lattice for a Wide Energy Range," in *Proc. IPAC'22*, Bangkok, Thailand, 2022, pp. 1946–1949. doi:10.18429/JACoW-IPAC2022-WEPOPT042

[4] M. G. Signorelli, G. H. Hoffstaetter, and V. Ptitsyn, "Electron Polarization Preservation in the EIC," presented at the 14th Int. Particle Accelerator Conf. (IPAC'23), Venice, Italy, May 2023, paper MOPA052.

[5] D. Sagan, *The Bmad Manual*. 2022. https://www.classe.cornell.edu/bmad/manual.html

[6] D. Sagan, *The Tao Manual*. 2022. https://www.classe.cornell.edu/bmad/tao.html

[7] F. Schmidt, E. Forest, and E. McIntosh, "Introduction to the polymorphic tracking code: Fibre bundles, polymorphic Taylor types and "Exact tracking"," CERN, Tech. Rep. CERN-SL-2002-044-AP, KEK-REPORT-2002-3, 2002. http://cds.cern.ch/record/573082

[8] A. Wolski, "Alternative approach to general coupled linear optics," *Phys. Rev. ST Accel. Beams*, vol. 9, p. 024 001, 2006. doi:10.1103/PhysRevSTAB.9.024001

[9] C. Gulliford and A. Bartnik, "Demonstration of cathode emittance dominated high bunch charge beams in a dc bun-based photoinjector," *Appl. Phys. Lett.*, vol. 106, p. 094 101, 2015.

[10] D. Sagan, *Long Term Tracking Program*. 2022. https://www.classe.cornell.edu/bmad/manuals/long_term_tracking.pdf